The Hydrodynamic Drag of Full Scale Trees

C.A.M.E. Wilson & P. Xavier
Hydro-environmental Research Centre, School of Engineering, Cardiff University, UK

T. Schoneboom & J. Aberle
Leichtweiß-Institut für Wasserbau, TU Braunschweig, Braunschweig, Germany

H.-P. Rauch & W. Lammeranner & C. Weissteiner
Institute of Soil Bioengineering and Landscape Construction, University of Natural Resources and Applied Sciences, Vienna, Austria

H. Thomas
Forest Research, Talybont Research Office, Powys, UK

ABSTRACT: This paper presents selected results from a laboratory study which was carried out under the EU Hydralab III programme in a 320 m long towing tank at the CEHIPAR ship canal facility in El Pardo, Madrid. Hydrodynamic drag-velocity relationships were determined for a total of 22 full-scale trees of three different genera (*Salix sp.*, *Alnus glutinosa* and *Populus alba*) of height between 1.4 and 4 metres. In this paper, preliminary results for nine *Salix* specimen are presented. One of the main objectives of this study is to examine these drag-velocity relationships at high resolution and therefore relate the tree's behaviour under flow action to (i) its physical attributes and (ii) different stages of streamlining. It was found that at the lowest velocities (between zero and 0.5 m/s) the drag force-velocity variation approached the squared relationship expected for a bluff body as described by the classical drag force equation. At higher velocities (over approximately 0.5 m/s) the force was found to vary linearly with velocity. For the selection of results presented here, the percentage contribution to drag from spring leaves and flowers was found to vary from 24.4 % to 54.8 % within this linear range. The linear drag-area coefficient (the product of the drag coefficient and the frontal projected area) was determined for all specimen within the zone of linear variation between drag force and velocity. Although the dataset is limited it was found that dry mass and volume of trees were positively correlated to the linear drag-area coefficient.

Keywords: Vegetation, Salix, Leaves, Drag Force

1 INTRODUCTION

It is increasingly recognised that the current reliance on engineered flood protections to defend all areas against future flooding is not sustainable. Instead, attention is shifting towards integrated approaches considering the whole catchment to manage flood risk. Land management and the use of forestation may be seen as having a significant contribution to make, particularly where engineered flood defences cannot be justified on cost-benefit grounds, but also to improve the effectiveness of existing defences against climate change. This is consistent with the delivery of an ecosystem services approach to securing a healthy environment.

By increasing the hydraulic roughness on a wide floodplain, woodland may have the potential to attenuate the flood hydrograph and delay the passage of floodwaters to downstream towns and cities. Woodland can also help to reduce flood flows through increased evapotranspiration and enhanced soil infiltration. The targeted restoration or creation of woodland, including energy plantations, could make a major contribution to protecting rural and urban communities from future flooding, as well as delivering a wide range of other benefits such as carbon sequestration, biodiversity, recreation and improved water quality.

River modelling software and computational fluid dynamics codes are effective and widely used tools in determining river water levels and velocities, particularly in the prediction of high flow events which may endanger life or property (e.g., Pender 2006). However, the modelling of flows through riparian forests is hampered by a lack of data relating to the hydrodynamics of trees and shrubs under fluid action. At a time when the wide-ranging benefits of river restoration and reforestation are increasingly recognized in terms of ecological and climatic benefits (IPCC 2007; UN 2009), it is critical that the understanding of vegetated flows keeps pace with the continuous improvements in the numerical methods used to model free surface flows.

From the earliest approaches and numerical river models, vegetation has been modelled as an extension of boundary skin friction using roughness factors such as Manning's n or the Chezy factor (Chow 1959). However it has been shown that for vegetation that extends throughout the whole water column, bed boundary roughness coefficients such Manning's n vary as a function of flow depth (e.g., Ree 1958). A more appropriate model for representing the hydraulic resistance exerted by a single and/or a group of trees or shrubs is taking into account their hydrodynamic drag (e.g., Li & Shen 1973; Petryk & Bosmajian 1979). In the field of vegetation modelling, this has generally been accomplished on the basis of the classical drag formula (e.g., Hoerner 1965):

$$F_x = \frac{1}{2}\rho C_d A_p U^2 \qquad (1)$$

where F_x is the drag force exerted on the vegetation, ρ is the fluid density, C_d is the drag coefficient (in turbulent flows this relates to the shape of the obstacle and is a function of obstacle Reynolds-number), A_p is the projected area of the obstacle and U is the free stream velocity. Applying equation (1) to natural vegetation elements it is often assumed that the plants behave similar as rigid circular cylinders and that the drag coefficient C_d is constant in the order of magnitude around unity.

However, several studies (e.g., Oplatka 1998; Armanini et al. 2005; James et al. 2008; Wilson et al. 2008) showed that the application of equation (1) is hampered when being applied to natural vegetation as it is difficult to account for the tree's flexibility under flow action. In fact, for flexible vegetation elements it has been shown that the trunk and its branches reconfigure and streamline with increasing velocity (e.g., Oplatka 1998). This process causes the projected area and the drag coefficient to vary as a function of the velocity and shows that the simulation of natural vegetation by rigid cylinders is only a crude approximation of the reality and may only be valid for certain vegetation types such as reeds and or rigid tree trunks (e.g., Järvelä 2006).

Several authors have determined the drag coefficient of flexing trees through direct drag force measurements (e.g., Mayhead 1973; Fathi-Maghadam & Kouwen 1997; Oplatka 1998; Freeman et al. 2000; Armanini et al. 2005; Kane & Smiley 2006; Wilson et al. 2008). Oplatka (1998) tested natural trees in a towing tank and reported that, for velocities greater than 1 m/s, the force varies linearly with velocity. This is thought to be due to the significant decrease in projected area of the tree as it flexes longitudinally and laterally under flow action and is in contrast to the quadratic drag force relationship expected for a rigid body (equation 1).

However, the observed linear relationships have, in general, been based on few data points. For example Oplatka (1998) investigated the drag force-velocity relationship at velocities of 1 m/s and above at increments of 0.5 m/s. The flexing behaviour and force-velocity relationship below this value was not reported.

Due to the difficulties involved in measuring the physical parameters of trees and the large population sample needed in order to make definitive conclusions, few researchers have quantified and related physical plant parameters to the drag exerted. Some authors, including Rudnicki et al., (2004) and Vollsinger (2005) studied the relationship between crown mass and drag exerted on trees in wind tunnels, finding that the drag was proportional to the crown mass, wind speed and crown size.

On the other hand, several researchers have characterized the force-velocity behaviour of a flexible plant and the associated influence of the variation in the projected area of the vegetation under flow action, through the drag-area parameter $C_d A_P$, the product of drag coefficient and projected area (e.g., Armanini et al. 2005; Wilson et al. 2008). In this manner the classical drag formula shown in equation (1) was used to evaluate the product $C_d A_P$ for each velocity examined as the drag coefficient and projected area are both functions of velocity.

The experimental programme on which this study is based is a first step towards further understanding how the physical characteristics of flexing trees relate to the hydrodynamic drag. The results presented in this paper are part of a wider series of experiments undertaken to investigate the hydrodynamic drag imposed by full scale trees with and without foliation. In total, 22 full-scale trees of three different genera (*Salix*, *Alnus* and *Populus*) of height between 1.4 and 4 meters were tested. Here, we concentrate on presenting the results from tests conducted on nine trees of the genus *Salix* where data was recorded at velocity increments of 0.06 m/s to 0.50 m/s, allowing examination of the drag-velocity relationship in greater detail than previously observed. Furthermore, we attempt to understand the linkage between hydrodynamic drag and a tree's physical properties.

2 METHODOLOGY

The experiments were conducted at the 320 m long, 12.5 m wide and 6.5 m deep CEHIPAR ship canal facility in El Pardo, Madrid in March and

April 2008 under the Transnational Access Activities EU Hydralab III scheme. The facility and the carriage which housed an operations room is shown in Figure 1.

Figure 1: CEHIPAR Ship Canal Facility. The upper photograph shows the canal and the lower photograph the carriage on rails suspended over the canal.

In order to measure drag forces exerted by the trees they were attached upside-down to a dynamometer suspended beneath the carriage spanning the canal width. The tree orientation was selected according to the direction of the tree's tendency to bend while upright. In this way, the bending during testing worked with the natural curvature. The carriage moved along canal-side railings and its velocity was controlled from the operations room to an accuracy of 1 mm/s. The carriage movement was bi-directional and this enabled drag force measurements while the carriage moved along the canal in both directions. During the experiments, this was taken into account by rotating the tree on arrival at the end of the canal through 180°. The direction of the carriage motion will be referred hereafter as a forward run (moving away from the start of the canal to the end of the canal) and a backward run (moving from the canal end to the start of the canal). The carriage rested for a period of a few minutes between the forward and backward runs. This was to ensure that the basin waves generated during each run were sufficiently dissipated and would not affect the data collected. The forces in three directions on the dynamometer were monitored in real time to an accuracy of 0.0098 N.

To verify the accuracy and performance of the drag force measurement system and to provide a baseline with which to compare the tree results, the drag force-velocity relationship was determined for a solid steel cylinder of diameter 30 mm as a first step (not shown here). To ensure repeatability of results, each experiment was carried out twice with both a forward and a backward run.

During a single forward or backward run, force measurements were taken for several velocities in succession. An example of a time-series for velocities in the range of 0.25 to 1.75 m/s is shown in Figure 2. All three force components are shown; F_x, F_y and F_z refer to the force components in the longitudinal, lateral and vertical directions, respectively. Figure 2 shows that the force reached a peak at the transition point between two subsequent velocities where the carriage accelerated. The acceleration and hence the change in velocity was reached in a few seconds. It is clear however that the change in force exerted on the dynamometer continued to change for a much longer period due to plant reconfiguration. This can be seen on the declining force magnitude following the acceleration and it was observed that this effect became more significant at the higher velocities examined.

In order to ensure that representative force measurements are derived from the time-series dataset, a statistical analysis was carried out to find the optimum time segment based on the cumulative average and standard deviation calculations. Considering the acceleration, deceleration and the stabilization of the tree configuration, this analysis was carried out from the end to the beginning of a velocity step (i.e. just before the next velocity increase). This procedure resulted in a maximum time segment of 20 seconds at the end of a velocity step for the time-averaging process.

In order to relate physical characteristics of the trees to the resultant drag, physical properties of the woody parts of the trees were measured and documented in quartile heights, including height, diameter, mass and volume. To determine the contribution to drag from the presence of leaves and flowers (catkins), the mass and volume, and dry mass fraction (the combined leaf and flower mass expressed as a percentage of total tree mass) were also determined. It should be noted that we did not distinguish between leaves and flowers when calculating the dry mass fraction. The experiments were performed during early spring and consequently the leaf size and leaf to wood ratio were relatively low compared to later in the season, although the presence of flowers contributed significantly to the dry mass fraction and the overall increase in drag.
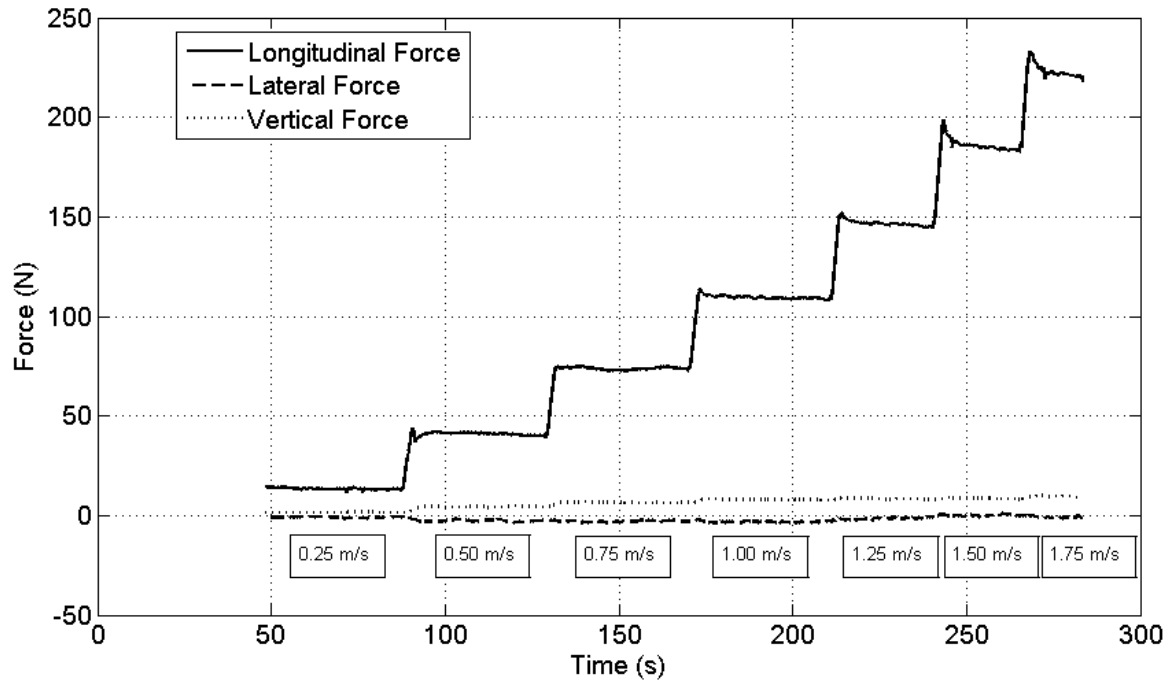
Figure 2 Time-series of force components measured for a succession of velocities.

3 RESULTS

Figure 3 presents the longitudinal drag force variation with velocity for the *Salix* trees both with and without leaves and flowers. The figure indicates that above a threshold velocity (U_T) of approximately 0.5 m/s, the variation of force with velocity is apparently linear for the majority of trees in both conditions. Assuming such a linear behaviour for the high velocity data, the velocity threshold U_T was determined from the intersection point between a linear regression fit applied to the high velocity data and a second-order regression fit applied to the lower velocity data. The subjectively chosen governing condition to identify the linear region was that the squared correlation coefficient R^2 must be greater than 0.99 for the linear regression. The velocity thresholds (U_T) for the trees with and without leaves and flowers are presented in Table 1.

Table 1. Velocity thresholds U_T. (F-With leaves and flowers, NF-No leaves or flowers)

Salix	1	2	4	8	10	11	12
F U_T (m/s)	0.62	0.33	0.47	0.34	0.36	0.91	0.50
NF U_T (m/s)	0.49	0.42	0.49	0.38	0.38	0.30	0.51

We note that this method was difficult to apply to *Salix* 3 which was not tested at high enough velocities to obtain a value for the velocity threshold and *Salix* 9, where the non-linear rate of increase

of force with velocity appears to continue to rise until over 3.5 m/s (Figure 3a).

It was mentioned above that the drag-area parameter C_dA_p based on the rigid body model can be used to characterize the drag-velocity behaviour of a flexible body. Here we define a modified version referred to as the 'linear drag-area coefficient' for a flexible body when the drag-force relationship is linear. The linear drag-area coefficient is based on the gradient of the force-velocity curve in the flexing zone and is defined as:

$$C_d A_p U_0 = \frac{2\Delta F_x}{\rho \Delta U} \qquad (2)$$

where ΔF_x and ΔU_0 refer to the change in longitudinal drag force and the change in the longitudinal velocity respectively. U_0 is a velocity parameter to maintain dimensionality validity. The terms on the L.H.S. of equation (2) together form the composite linear drag-area coefficient term. While the individual value and magnitude of U_0 is not explored here, it will be the subject of future research. According to the identified linear relationship, the linear drag-area coefficient $C_dA_pU_0$ is constant for all velocities in the flexing zone and therefore each tree can be characterized by a single value within this zone. The $C_dA_pU_0$ parameter has an advantage over the previously defined drag-area parameter as it encompasses all the drag and flexing effects of a tree specimen over a range of velocities instead of considering one single velocity.
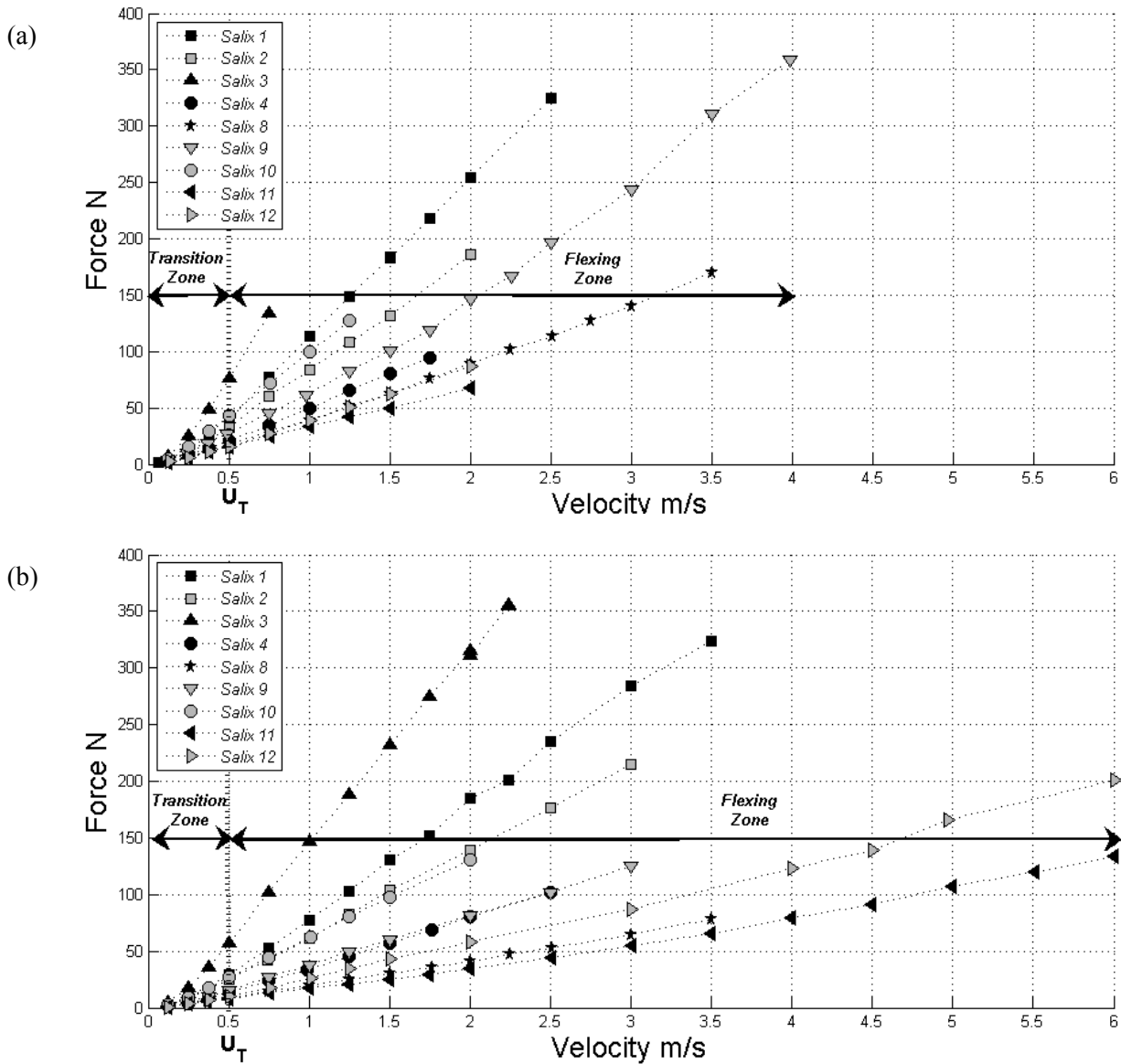
Figure 3: Variation of drag force with velocity for *Salix* trees, (a) with leaves and flowers and (b) without leaves and flowers.

$C_dA_pU_0$ is shown in Figure 4 as a function of various physical tree characteristics. Figures 4 (a) and (b) present $C_dA_pU_0$ as a function of the tree diameter at the first quartile height (as measured from the base of the tree) and the mid-length diameter and Figures 4 (c) and 4 (d) present $C_dA_pU_0$ as a function of the tree dry mass and volume. The data point in the top right corner of all the Figure 4 plots corresponds to *Salix* 3, a specimen which was considerably greater in mass and height than the other specimens.

The linear fit equation was used to parameterise the force-velocity relationship in the flexing zone. The comparison of the results with leaves and flowers against those without enabled the determination of the mean contribution to drag from the presence of the leaves and flowers for each tree. The dry mass fraction of the leaves and flowers and the equivalent percentage contribution to drag for the *Salix* trees are presented in Table 2. We note that tree *Salix* 3 was not tested at sufficient velocities above 0.5 m/s with leaves and flowers and that the leaf and flower mass for tree *Salix* 9 was not recorded. Therefore these data could not be included in Table 2.

Table 2. Leaf and flower dry mass fraction and drag contribution due to the presence of leaves and flowers

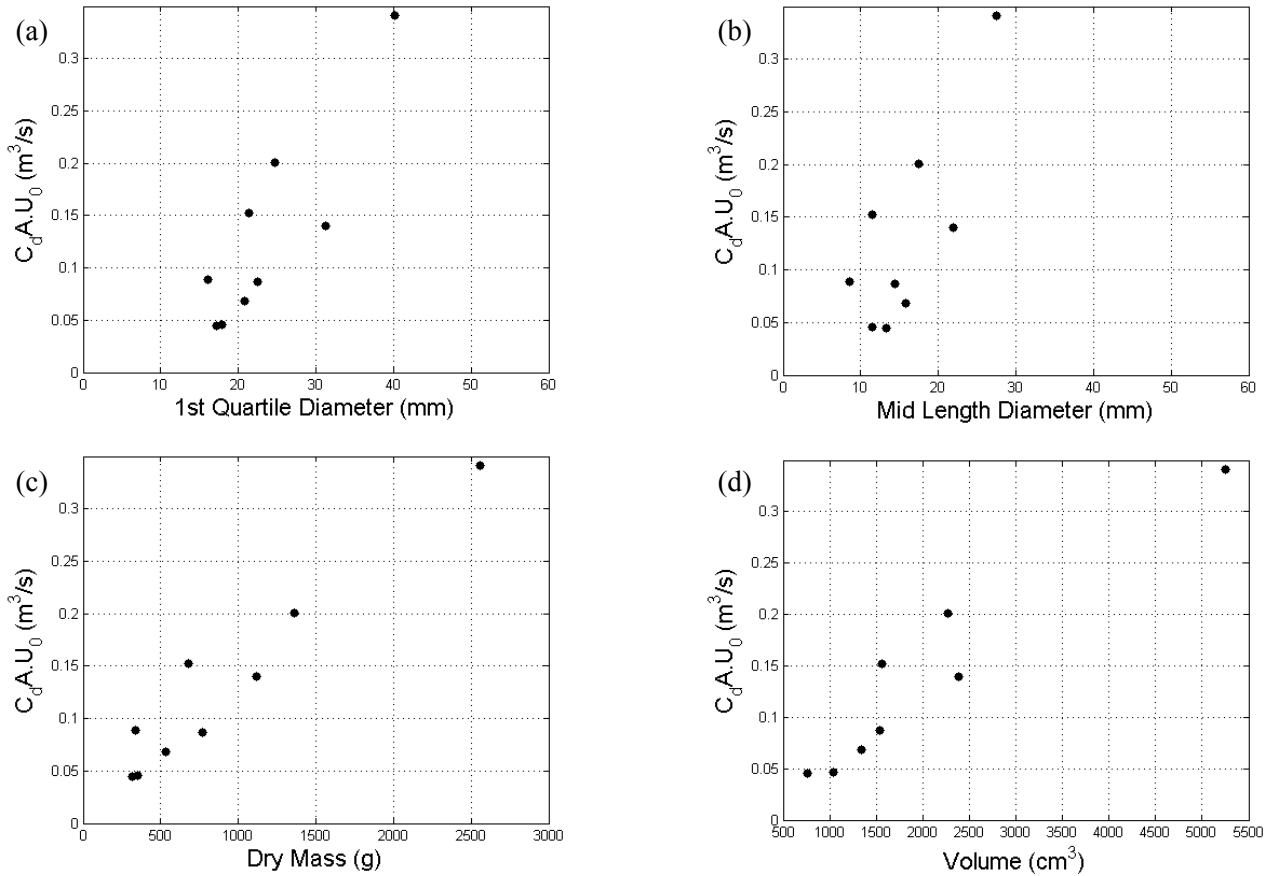| Salix	1	2	4	8	10	11	12
Mass fraction (%)	3.1	2.5	8.5	21.0	7.0	12.8	8.6
Drag (%)	28.8	24.7	24.4	54.8	37.8	33.7	27.3

Figure 4: Relationship of linear drag-area coefficient against (a) first quartile diameter (b) mid length diameter c) dry mass and (d) volume.

4 DISCUSSION

The drag force variation with velocity results shown in Figure 3 confirm the experience of previous studies investigating flexing trees, but show an increased accuracy and data resolution. The relatively large number of measurements taken at velocities below 1 m/s, compared to previous studies, demonstrates that there are two zones of drag-velocity behaviour. By determining the value of U_T beyond which the tree displays a linear variation of force with velocity, the data for any given tree can be divided into two zones. The *transition zone* is bounded by the very lowest velocities tested, when the deflection of the tree is negligible and the tree can be assumed to act as a rigid body, until the threshold velocity U_T is reached. In this zone, there is a gradual transition from the tree acting as a rigid body to one acting as a fully responsive flexing body. A similar behaviour for flexible vegetation elements was described in the study of Schoneboom & Aberle (2009) for flexible artificial vegetation elements.

In the *flexing zone*, which is bounded by U_T and the maximum velocities tested the tree

streamlines, regardless of whether or not the tree has leaves and flowers. Streamlining causes the projected tree area to decrease with increasing velocity. It appears that the linear drag-velocity relationship is reached at approximately 0.5 m/s (Figure 3, Table 1). The velocity at which U_T is reached for each tree is different depending on whether or not the tree has leaves and flowers. However, the U_T values provided in Table 1 indicate that a consistent variation in the magnitude of U_T between the tests is not existent. This issue will be investigated further in our future analyses taking into account the other 13 tested trees. Nonetheless, by determining the gradient of the assumed linear force variation with velocity in the flexing zone it was possible, with the exception of Salix 3 and Salix 9, to adequately characterise the drag force-velocity relationship of the trees at velocities above 0.5 m/s.

The contribution to drag force from the presence of leaves and flowers varied from 24.4 % to 54.8 % while the equivalent mass fraction of leaves and flowers varied from 2.5 % to 21 % (Table 2) showing that leaves and flowers contribute significantly to the drag (see also Vogel 1994). However, a larger sample of trees may be needed in order for the drag contribution of the

leaves and flowers to be related to the mass fraction.

In general, there is a positive correlation between the linear drag area coefficient and the diameter at the first quartile height and mid-height, dry mass and volume. There appears to be better correlation with dry mass and volume (Figures 4 (c) and (d)), compared to the first quartile and mid-height diameters. Hence, Figure 4 suggests that measurements of mass and volume are more indicative of the drag and flexing behaviour of the tree than a measurement of the main stem diameter.

The observed scatter in Figure 4 may be due to a number of factors. For example, several different species and sub-species were identified among the tested trees, with some more rigid than others. The trees all exhibited varying degrees of existing natural curvature and number and size of side branches, which may have additionally contributed to the wide spread of data points. This issue will also be further investigated analysing the total data set.

5 CONCLUSION AND FUTURE WORK

The drag force variation with velocity has been presented for *Salix* trees exhibiting spring leaves and flowers and for bare stem trees stripped of all leaves and flowers. It has been shown that the presence of leaves and flowers can significantly contribute towards the overall drag of a tree. The results obtained show a velocity-dependent variation in the response of the trees under flow action, with two zones identifiable, a transition zone and a flexing zone. The linear drag-velocity relationship was reached at approximately 0.5 m/s.

The relationship between linear drag-area coefficient $C_dA_pU_0$ and tree physical parameters of stem diameter, height and mass indicates that it is possible to obtain functional relationships to determine the resistance of flexible floodplain woodland vegetation through non-destructive measurement methods. It was found that the measurement of mass and/or volume was more indicative of the overall drag and flexing behaviour of a specimen than a measurement of the main stem diameter. Further analysis, taking into account the available additional data, is currently underway to analyse the video footage from the experiments in order to understand the contribution of tree form and structure to the drag-velocity relationship.

REFERENCES

Armanini, A., Righetti, M. & Grisenti, P. 2005. Direct measurement of vegetation resistance in prototype scale, *J. Hydraul. Res.*, 43(5), 481-487

Chow, V.T. 1959. *Open Channel Hydraulic*s, McGraw-Hill.

Fathi-Maghadam, M. & Kouwen, N. 1997. Nonrigid, non-submered, vegetative roughness on floodplains, *J. Hydraul. Eng.*, 123(1), 51-57.

Freeman, G.E., Rahmeyer, W.J. & Copeland, R.R. 2000. Determination of resistance due to shrubs and woody vegetation, *Technical report, US Army Corps of Engineers.*

Hoerner, S. (1965). *Fluid-Dynamic Drag,* Hoerner, S., Brick Town.

IPCC 2007. Climate change 2007 synthesis report, *Technical report, IPCC.*

Järvelä, J. 2006. Vegetative flow resistance: characterization of woody plants for modeling applications. In: R. Graham (ed), Proc. of the World Water and Environmental Resources Congress 2006. 21-25 May 2006, Omaha, USA, papers on CD-Rom.

James, C.S., Goldbeck, U.K., Patini, A., & Jordanova, A.A. 2008. Influence of foliage on flow resistance of emergent vegetation. *J. Hydraul. Res.*, 46(4), 536-542.

Kane, B. & Smiley, T. 2006. Drag coefficients and crown area estimation of red maple, *Can. J. For. Res.*, 38(6), 1275-1289.

Li, R.-M. & Shen, H.W. 1973. Effect of tall vegetations on flow and sediment, *J. Hydraul. Div.*, 99(HY5), 793- 814.

Mayhead, G.J. 1973. Some drag coefficients for British forest trees derived from wind tunnel studies. *Agricultural Meteorology*, 12, 123-130.

Oplatka, M. 1998. Stabilität von Weidenverbauungen an Flussufern, *PhD thesis*, ETH Zürich.

Pender, G. 2006. Briefing: Introducing the Flood Risk Management Research Consortium." *Water Management*, 159(WM1), 3-8.

Petryk, S. & Bosmajian, G.I. 1975. Analysis of flow through vegetation, *J. Hydraul. Div.*, 101(HY7), 871-884.

Ree, W.O. 1958. Retardation coefficients for row crops in division terraces, *Trans. Am. Soc. Agric. Eng.*, 1, 78- 80.

Rudnicki M., Mitchell S.J. & Novak M.D. 2004. Wind tunnel measurements of crown streamlining and drag relationships for three conifer species. *Can. J. For. Res.*, 34(3), 666-676.

Schoneboom, T. & Aberle, J. 2009. Influence of foliage on drag force of flexible vegetation. 33rd IAHR Congress, Vancouver, Canada, Papers on CD-Rom.

UN 2009. State of the world's forests 2009, Technical report, Food and Agriculture Organization of the United Nations.

Vogel, S. 1994. *Life in moving fluids: the physical biology of flow*. 2nd edition, Princeton, Princeton University Press.

Vollsinger S., Mitchell S.J., Byrne, K.E., Novak, M.D. & Rudnicki, M. 2005. Wind tunnel measurements of crown streamlining and drag relationships for several hardwood species. *Can. J. For. Res.*, 35(5), 1238-1249.

Wilson, C., Hoyt, J. & Schnauder, I. 2008. Impact of foliage on the drag force of vegetation in aquatic flows. *J. Hydraul. Eng.*, 134(7), 885-891.